

Polarization-Current-Based FDTD Near-to-Far-Field Transformation

Yong Zeng and Jerome V. Moloney

Arizona Center for mathematical Sciences, University of Arizona, Tucson, Arizona 85721

**Corresponding author: zengy@acms.arizona.edu*

A new near-to-far-field transformation algorithm for three-dimensional finite-difference time-domain is presented in this article. This new approach is based directly on the polarization current of the scatterer, not the scattered near fields. It therefore eliminates the numerical errors originating from the spatial offset of the E and H fields, inherent in the standard near-to-far-field transformation. The proposed method is validated via direct comparisons with the analytical Lorentz-Mie solutions of plane waves scattered by large dielectric and metallic spheres with strong forward-scattering lobes. © 2018 Optical Society of America

The grid-based finite-difference time-domain (FDTD) method is one of the most popular Maxwell solvers, which has been proven to be efficient, stable and easy-to-implement [1]. Due to the computational resource limitation, a FDTD simulation truncates the open boundary to a spatial domain adjacent to the scatterer. The near-to-far-field (NTFF) transformation, therefore, is routinely employed to obtain the far-zone information such as antenna scattering patterns and nanocavity radiation patterns [1–8]. The standard NTFF (S-NTFF) transformation, introduced in the early 1980s, is based on the vector Kirchhoff integral relation [1]. The scattered fields in the far zone are calculated through an integration of the near-zone fields over a virtual closed (Huygens) surface completely enclosing the scatterer [9]. To accomplish this we need compute, via FDTD and discrete Fourier transformation, the scattered E and H fields tangential to the fictitious surface. However, the spatial and temporal offset between E and H field, a character of the Yee update scheme [1], may result in unacceptable numerical errors [10–12]. For instance, Ref. [13] demonstrated that the accuracy of the S-NTFF is unacceptable when calculating the backscattering from strongly forward-scattering objects, and the relative error may be as high as two orders of magnitude at short wavelength. To improve its numerical accuracy, at least two different modifications have been proposed, including discarding information in the forward-scattering region [13] and using geometric mean in place of arithmetic mean [14].

In classical electrodynamics, the optical response of medium made up of a large number of atoms or molecules originates from the perturbed motions of the charges bound in each molecule. The molecule charge density is distorted by the external electromagnetic fields, and further produces an electric polarization \mathbf{P} in the medium [9]. Consequently in this article we proposal using the polarization current, rather than the scattered near fields, to derive the far-zone information. The proposed approach is validated via comparison with rigorous analytical solutions of plane wave scattered by large dielectric and metallic spheres. A detailed discussion regarding its advantages and disadvantages is also presented.

In the absence of sources, the Maxwell equations are read as

$$\begin{aligned}\nabla \cdot \mathbf{B} &= 0, & \nabla \times \mathbf{E} &= -\frac{\partial \mathbf{B}}{\partial t}, \\ \nabla \cdot \mathbf{D} &= 0, & \nabla \times \mathbf{H} &= \frac{\partial \mathbf{D}}{\partial t}.\end{aligned}\quad (1)$$

Assuming the following constitutive relations $\mathbf{D} = \epsilon_0 \mathbf{E} + \mathbf{P}$ as well as $\mathbf{B} = \mu_0 \mathbf{H}$ (the scatterer is therefore nonmagnetic), we arrive an inhomogeneous Helmholtz wave equation for the vector potential \mathbf{A} in the Lorentz gauge [9]

$$\nabla^2 \mathbf{A} - \frac{1}{c^2} \frac{\partial^2 \mathbf{A}}{\partial t^2} = -\mu_0 \mathbf{J}(t), \quad (2)$$

where \mathbf{J} is the polarization current defined as $\mathbf{J} = \partial \mathbf{P} / \partial t$ [15]. With a time dependence $e^{-i\omega t}$ understood, Eq. (2) becomes

$$\nabla^2 \mathbf{A} + k^2 \mathbf{A} = -\mu_0 \mathbf{J}(\omega), \quad (3)$$

with $k = \omega/c$ being the vacuum wave number. A formal solution of the above equation, with the help of free-space Green function, can be written as [9]

$$\mathbf{A}(\mathbf{r}) - \mathbf{A}^{(0)}(\mathbf{r}) = \frac{\mu_0}{4\pi} \int_v \mathbf{J}(\mathbf{r}') \frac{e^{ik|\mathbf{r}-\mathbf{r}'|}}{|\mathbf{r}-\mathbf{r}'|} d\mathbf{r}'. \quad (4)$$

The left-hand side represents the scattered wave with $\mathbf{A}^{(0)}$ representing the incident wave. To obtain the field in the radiation zone, it is sufficient to approximate the numerator with [9]

$$|\mathbf{r} - \mathbf{r}'| \approx r - \mathbf{n} \cdot \mathbf{r}', \quad (5)$$

while in the denominator $|\mathbf{r} - \mathbf{r}'| \approx r$. Here \mathbf{n} is a unit vector in the direction of \mathbf{r} . The far-zone vector potential of the scattered field is therefore expressed as

$$\lim_{r \rightarrow \infty} \mathbf{A}(\mathbf{r}) \approx \frac{\mu_0 e^{ikr}}{4\pi r} \int_v \mathbf{J}(\mathbf{r}') e^{-ik\mathbf{n} \cdot \mathbf{r}'} d\mathbf{r}' \equiv \frac{\mu_0 e^{ikr}}{4\pi r} \mathbf{p}. \quad (6)$$

It behaves as an outgoing spherical wave while depends on the polar and azimuth angles (θ, ϕ) in spherical polar coordinate. The scattered fields in the radiation zone, keeping only the leading order, are further given as

$$\mathbf{B} = \frac{ik\mu_0}{4\pi r} e^{ikr} \mathbf{n} \times \mathbf{p}, \quad \mathbf{E} = c\mathbf{B} \times \mathbf{n}. \quad (7)$$

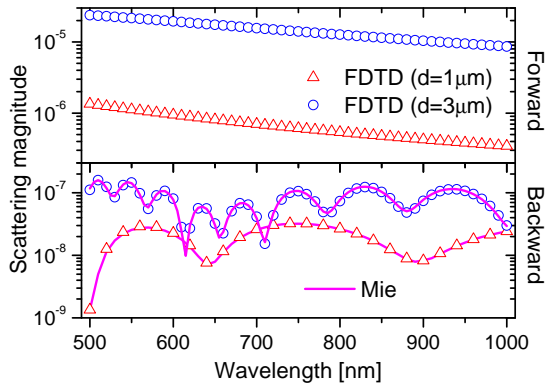


Fig. 1. Forward and backward scattering magnitudes of 1- μm and 3- μm diameter dielectric spheres with $\epsilon_r = 1.21$. Both numerical FDTD solution and rigorous Lorentz-Mie solution are presented. The cell size employed in FDTD simulation is 25 nm. The corresponding S-NTFF results can be found from Fig.1 of Ref. [13].

Evidently, both fields are transverse to the radius vector \mathbf{n} and fall off as r^{-1} .

The time-averaged power scattered per unit solid angle is

$$\frac{dP}{d\Omega} = \frac{1}{2} \text{Re} \left[r^2 \mathbf{n} \cdot \mathbf{E} \times \mathbf{H}^* \right] = \frac{k^2 \eta_0}{32\pi^2} |(\mathbf{n} \times \mathbf{p}) \times \mathbf{n}|^2 \quad (8)$$

with $\eta_0 = \sqrt{\mu_0/\epsilon_0}$ being the intrinsic impedance of free space. To obtain the scattering cross section, the scattered power needs be normalized to the incident power [9]. It is worth noting that the above general expression is quite similar to that of an oscillating electric or magnetic dipole, except that the $\mathbf{p}(\mathbf{n})$ here is angular-dependent [9].

The above derivation immediately implies two features of our approach: (1) It depends only on the polarization current \mathbf{J} but not the scattered electromagnetic fields \mathbf{E} and \mathbf{H} , the error induced by the spatial offset between them in the S-NTFF is therefore completely avoided; (2) Unlike the S-NTFF, there is no requirement of scattered fields. Consequently, our approach is easier to implement for strongly convergent light sources such as Gaussian beam [16].

It should be emphasized that we can very easily extract the polarization current from FDTD, because an auxiliary differential equation of the current is frequently adopted by standard FDTD to simulate dispersive, nonlinear and even quantum-mechanical media [1]. For the special case of a dielectric scatterer, the standard FDTD itself is enough to provide the information of the current, since it connects to the electric field as $\mathbf{J}(\omega) = -i\omega\epsilon_0\chi\mathbf{E}(\omega)$ with χ being the susceptibility.

To validate our approach as well as the corresponding numerical algorithm, we begin by considering the backscattering from two strongly forward-scattering dielectric spheres with

a relative permittivity $\epsilon_r = 1.21$ ($\chi = 0.21$) which were considered in Ref. [13, 14] with the use of the (modified) S-NTFF. Assuming the incident field propagates along the positive x direction, the backscattering (corresponding to $\mathbf{n} = (-1, 0, 0)$) power is simply given as

$$\frac{k^2 \eta_0}{32\pi^2} [|p_y(\mathbf{n})|^2 + |p_z(\mathbf{n})|^2], \quad (9)$$

that is, we do not need consider the x -component current. In our simulations, the FDTD lattice is terminated by a uniaxial perfectly matched layer (UMPL) in all directions [1], and the whole computational space is divided into uniform cubic cells with size of 25 nm. Furthermore, an impulsive wideband plane wave is excited to obtain the spectra in the wavelength domain 500-1000 nm.

Fig.1 presents the FDTD calculated far-field spectra for two spheres with diameters $d = 1\mu\text{m}$ and $d = 3\mu\text{m}$. Because their sizes are on the order of incident wavelength, the appearance of higher-order multipoles distort the symmetrical electric-dipole pattern and result in strong forward scattering. The biggest contrast between forward and backward scattering appears for the $1\mu\text{m}$ -diameter sphere. At 500-nm wavelength, its scattering in the forward direction is almost three orders of magnitude stronger than its backward counterpart. As a reference, the analytical Lorentz-Mie solutions are also shown. Clearly, excellent agreement is achieved even when the incident wavelength is coarsely resolved on the FDTD grid. Under the same conditions, the relative error of the S-NTFF result is as high as two orders of magnitude [13], and modifications such as the geometric mean must be introduced to improve its numerical accuracy [14].

We further consider the scattering of a $1\mu\text{m}$ -diameter gold sphere with Drude-type permittivity approximated as

$$\epsilon(\omega) = 1.0 - \frac{\omega_p^2}{\omega(\omega + i\gamma)} \quad (10)$$

in the wavelength region 700-1200 nm. The bulk plasma frequency ω_p is taken as $1.367 \times 10^{16} \text{s}^{-1}$, and the phenomenological collision frequency $\gamma = 6.478 \times 10^{13} \text{s}^{-1}$ [17]. Because of the negative permittivity, surface plasmon polaritons (SPP) are excited and the resulting evanescent waves concentrate around the metallic surface. To simulate these nonpropagating fields, sufficiently finer resolution is needed in FDTD to achieve acceptable accuracy. Fig.2 shows the comparison of the analytical Lorentz-Mie solution with our FDTD numerical results (with cell size of 10 nm). Clearly, they are quite close, except tiny blue shifts of SPP resonances as well as a relative difference of roughly 5% around the 770-nm wavelength. It should be emphasized that these disagreements are induced by the inherent staircasing of the standard FDTD on a Cartesian grid and not due to our NTFF. In the simulation the diameter of the metallic sphere is resolved by 100 cells, and better agreement can be achieved by decreasing the cell size.

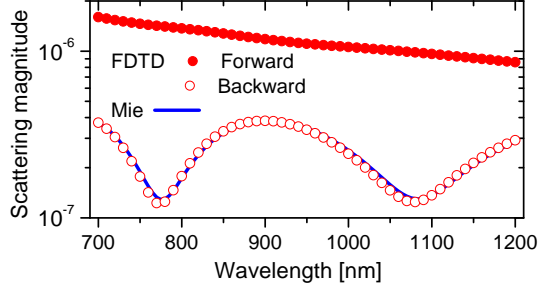


Fig. 2. Far-field scattering spectra of $1\mu\text{m}$ -diameter gold sphere. Both numerical FDTD solution and rigorous Lorentz-Mie solution are presented. The cell size employed in FDTD simulation is 10 nm .

The key differences between our current-based NTFF with the S-NTFF can be summarized as follow: (1) Origins of numerical errors are different. They both suffer from staircasing. However, the S-NTFF has two more sources including the scattered-field requirement (we thus need total field/scattered field or pure scattered field scheme [1]) and the spatial offset of the E and H fields over the integral surface [13,14]; (2) A virtual integral surface enclosing the whole scatterers is not needed in our approach. It is therefore easily and efficiently implemented within the framework of standard FDTD codes; (3) The two methods have different computational burdens. Consider a cubic scatterer resolved by N^3 cells, the total number of discrete Fourier transformations to be performed is $3 \times N^3$ in volume integration (our method) in comparison with $12 \times N^2$ in surface integration (S-NTFF). On the contrary, a multiple scatterer cluster with small volume but large surface may require more calculational resources in the S-NTFF; (4) The current-based NTFF has a close relation with the analytical multipole expansion, it is therefore convenient to identify the contributions from different multipolar sources and further provide insights into complex electromagnetic processes including radiation, diffraction and scattering [5,9].

It should be pointed out that the spatial offset between E and H field can be avoided by using the scalar Kirchhoff integral formula

$$\psi(\mathbf{r}) = -\frac{1}{4\pi} \int_S \frac{e^{ikR}}{R} \left[\nabla' \psi + ik \left(1 + \frac{i}{kR} \right) \frac{\mathbf{R}}{R} \psi \right] \cdot d\mathbf{s} \quad (11)$$

with $\mathbf{R} = \mathbf{r} - \mathbf{r}'$ and ψ being any component of \mathbf{E} or \mathbf{H} [9]. However, the integral surface S generally is infinite for an open-boundary problem. To achieve acceptable accuracy in numerical simulation, we need to truncate it to a finite surface with sufficient area. Consider an electric dipole with size a . The radius of the integral surface should be roughly $10a$ to contain the field with amplitude bigger than 10% of the dipole magnitude. It thus increases the computational burden.

To conclude, a polarization-current-based near-to-far-field transformation for the three-

dimensional finite-difference time-domain algorithm is developed. Because it completely eliminates the spatial-offset error inherent in the surface integration of standard near-to-far-field scheme, the new method can achieve improved accuracy even with coarse grids. Its validity and efficiency is further demonstrated via direct comparisons with analytical theory by calculating the backscattering from strongly forward-scattering objects including dielectric and metallic spheres. We also compare it to the standard near-to-far-field transformation in terms of calculational cost and accuracy. The new method may have potential applications in biophotonics and nanophotonics.

The authors thank Prof. Masud Mansuripur, Prof. Moysey Brio and Dr. Colm Dineen for their invaluable discussions. This work is supported by the Air Force Office of Scientific Research (AFOSR), under Grant No. FA9550-07-1-0010 and FA9550-04-1-0213. J. V. Moloney acknowledges support from the Alexander von Humboldt foundation.

References

1. A. Taflove and S. C. Hagness, *Computational Electrodynamics: the finite-difference time-domain method*, Third Edition, Artech House, 2005.
2. R. Drezek, A. Dunn, R. Richards-Kortum, *Appl. Opt.* 38, 3651 (1999).
3. S. Guo, S. Albin, *Opt. Express* 11, 1080 (2003).
4. R. Scott Brock, X-H Hu, P. Yang, J. Lu, *Opt. Express* 13, 5279 (2005).
5. C-C Oetting, L. Klinkenbusch, *IEEE Trans. Antennas Propag.* 53, 2054 (2005).
6. S-H Kim, S-K Kim, Y-H Lee, *Phys. Rev. B* 73, 235117 (2006).
7. T-D Onuta, M. Waegle, C. C. DuFort, W. L. Schaich, B. Dragnea, *Nano Lett.* 7, 557 (2007).
8. M. Husnik, M. W. Klein, N. Feth, M. König, J. Niegemann, K. Busch, S. Linden, and M. Wegener, *Nature Photon.* 2, 614 (2008).
9. J. D. Jackson, *Classical Electrodynamics*, Second Edition, John Wiley & Sons, 1975.
10. W. Sun, Q. Fu, *Appl. Opt.*, 39, 5569 (2000).
11. P. W. Zhai, Y. K. Lee, G. W. Kattawar, P. Yang, *Appl. Opt.* 43, 3738 (2004).
12. M. A. Yurkin, A. G. Hoekstra, R. S. Brock, Jun Q. Lu, *Opt. Express* 15, 17902 (2007).
13. X. Li, A. Taflove, V. Backman, *IEEE Antennas Wireless Propag. Lett.* 4, 35 (2005).
14. D. J. Robinson, J. B. Schneider, *IEEE Antennas Wireless Propag. Lett.* 55, 3204 (2007).
15. N. V. Budko, *Phys. Rev. Lett.* 102, 020401 (2009).
16. J. Lermé, C. Bonnet, M. Broyer, E. Cottancin, S. Marhaba, M. Pellarin, *Phys. Rev. B* 77, 245406 (2008).
17. E. D. Palik, *Handbook of optical constants of solids*, Academic, Orlando, 1985.

References

1. A. Taflove and S. C. Hagness, *Computational Electrodynamics: the finite-difference time-domain method* (Third Edition, Artech House, Boston, 2005).
2. R. Drezek, A. Dunn, and R. Richards-Kortum, “Light scattering from cells: Finite-difference time-domain simulations and goniometric measurements,” *Appl. Opt.* 38, 3651 (1999).
3. S. Guo and S. Albin, “Numerical techniques for excitation and analysis of defect modes in photonic crystals,” *Opt. Express* 11, 1080 (2003).
4. R. Scott Brock, X-H Hu, P. Yang, J. Lu, “Evaluation of a parallel FDTD code and application to modeling of light scattering by deformed red blood cells,” *Opt. Express* 13, 5279 (2005).
5. C-C Oetting, L. Klinkenbusch, “Near-to-far-field transformation by a time-domain spherical-multipole analysis,” *IEEE Trans. Antennas Propag.* 53, 2054 (2005).
6. S-H Kim, S-K Kim, Y-H Lee, “Vertical beaming of wavelength-scale photonic crystal resonators,” *Phys. Rev. B* 73, 235117 (2006).
7. T-D Onuta, M. Waegele, C. C. DuFort, W. L. Schaich, B. Dragnea, “Optical Field Enhancement at Cusps between Adjacent Nanoapertures,” *Nano Lett.* 7, 557 (2007).
8. M. Husnik, M. W. Klein, N. Feth, M. König, J. Niegemann, K. Busch, S. Linden, and M. Wegener, “Absolute Extinction Cross Section of Individual Magnetic Split-Ring Resonators,” *Nature Photon.* 2, 614 (2008).
9. J. D. Jackson, *Classical Electrodynamics*, Second Edition, John Wiley & Sons, 1975.
10. W. Sun, Q. Fu, “Finite-Difference Time-Domain Solution of Light Scattering by Dielectric Particles with Large Complex Refractive Indices,” *Appl. Opt.* 39, 5569 (2000).
11. P. W. Zhai, Y. K. Lee, G. W. Kattawar, and P. Yang, “Implementing the near to far-field transformation in the finite-difference time-domain method,” *Appl. Opt.* 43, 3738, (2004).
12. M. A. Yurkin, A. G. Hoekstra, R. S. Brock, Jun Q. Lu, “Systematic comparison of the discrete dipole approximation and the finite difference time domain method for large dielectric scatterers,” *Opt. Express* 15, 17902 (2007).
13. X. Li, A. Taflove, V. Backman, “Modified FDTD near-to-far-field transformation for improved backscattering calculation of strongly forward-scattering objects,” *IEEE Antennas Wireless Propag. Lett.* 4, 35 (2005).
14. D. J. Robinson, J. B. Schneider “On the use of the geometric mean in FDTD near-to-far-field transformations,” *IEEE Antennas Wireless Propag. Lett.* 55, 3204 (2007).
15. N. V. Budko, “Observation of Locally Negative Velocity of the Electromagnetic Field in Free Space,” *Phys. Rev. Lett.* 102, 020401 (2009).

16. J. Lermé, C. Bonnet, M. Broyer, E. Cottancin, S. Marhaba, M. Pellarin, “Optical response of metal or dielectric nano-objects in strongly convergent light beams,” *Phys. Rev. B* 77, 245406 (2008).
17. E. D. Palik, *Handbook of optical constants of solids*, Academic, Orlando, 1985.